

# COMPUTATIONAL AND EXPERIMENTAL STUDY OF A HELICOPTER TORSION ROTOR

Oleg Kirillov, Boris Kritsky, Ruslan Mirgazov, Vladimir Kulesh, Grigory Shvardygulov  
Central Aerohydrodynamic Institute (TsAGI), Russia

Viktor Anikin<sup>1,2</sup>

<sup>1</sup> VR-Technologies, <sup>2</sup> OJSC «KAMOV», Russia

## Abstract

A computational and experimental study of a helicopter torsion rotor is presented. The motion and deformation of the blade of a three-blade main helicopter rotor model were experimentally investigated. Measurements were carried out using a non-contact videogrammetry method using only one digital camera. The experimental data were approximated by Fourier series.

The flow around the rotor under experiment was simulated based on the unsteady vortex theory. In the calculations, rotor flapping relative to the horizontal hinge was considered. The difference in the flapping characteristics in case of hinged and torsion rotors is shown.

The results of numerical simulation of the flow around such a rotor as part of a coaxial system with different initial azimuths of the upper rotor blade relative to that of the lower rotor blade are presented. The effect of the initial mutual arrangement of the blades on the change in the rotor thrust coefficient and the thrust pulsation of a coaxial helicopter rotor is shown.

## 1. Introduction

Measurement of motion and deformation parameters of main rotor (MR) blades is one of the urgent problems of experimental aerodynamics and aeroelasticity.

Contactless optical methods prove to be the most promising for measuring the deformation of rotating objects due to their distinctive advantages: they are contactless, inertialess, highly informative and unlimited time resolution. These methods include videogrammetry methods (VGM) [1-3].

The optical VGM method was one of the solutions to the problem (1996) used to study the movement and deformation of full-scale helicopter rotor blades [1]. In this case, the considerable size of the study object (radius of 5–13 m) and relatively low angular rotational speeds (up to 350–380 rpm) allowed placing a digital camera on the rotor hub to optically superpose the camera's field of view with the blade under study. But to test models of rotors, tail rotors or smaller propellers, with a radius of up to 2.5 m, rotating at higher speeds of up to 10,000 rpm, placing the camera on the hub turned out to be technically inconvenient [2]. Therefore, another approach

was proposed and implemented - the VGM method with image convergence [2, 3], in which the camera was fixed motionless outside the experimental setup.

This paper discusses the use of the VGM method with image convergence for experimental study of the motion and deformation of the blade of a three-blade main rotor model fixed by means of an elastic torsion hinge.

The rotor flapping characteristics were also obtained by a numerical method based on the rotor vortex theory. The numerical study was conducted on the basis of the unsteady nonlinear rotor blade theory based on a thin bearing surface [4, 5].

## 2. Experimental setup

Motion parameters of a helicopter rotor blade were measured in the T-101 TsAGI wind tunnel using a rotor test rig. Figure 1 shows the experimental setup in the T-101 wind tunnel.

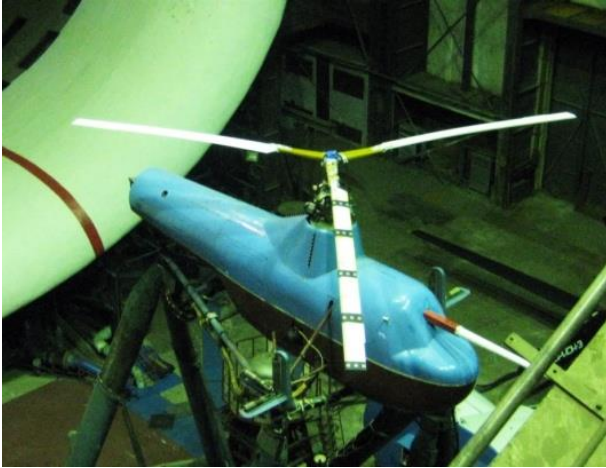
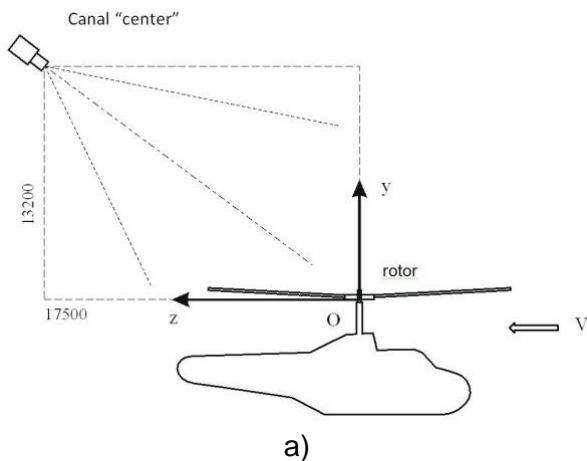
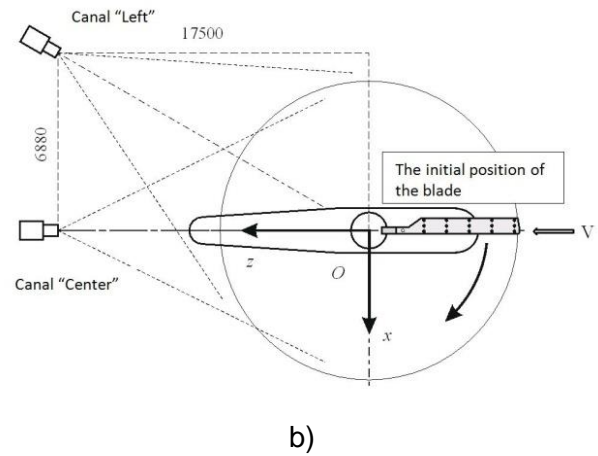


Fig.1 Experimental setup

A full-scale model of a three-blade torsion main helicopter rotor made of polymer composite materials was tested. The main technical characteristics of the rotor were as follows: diameter  $D=8.4$  m, chord  $c=0.206$  m, mass of the blade  $m=9.351$  kg, the planform shape was rectangular. For videogrammetry measurements, a grid of markers was applied to the upper surface of the selected blade (Fig. 1). The markers were made of retroreflective film and glued to the surface. The film with the adhesive layer was 0.12 mm thick. The measuring system was equipped with two identical videogrammetric channels - central (center) and left (Fig. 2, a and Fig. 2, b). The channels had the same structure with the same technical characteristics.



a)



b)

Fig. 2 Measuring system schematic

The digital camera of the central channel was installed above the T-101 wind tunnel diffuser about 13.2 m above the rotor rotation plane, approximately in the plane of symmetry of the helicopter test rig in the initial “zero” position, and that of the left channel was installed at the same level to the left at a distance of about 6.80 m from the first camera. The purpose of using two channels was to check the accuracy of measurements by comparing the results of two independent measurements.

In each VGM channel, the optical assembly comprised a digital camera and two LED lighting lamps with reflectors equivalent to an electrical power of 50 W each. In both channels, the same digital cameras were used, having a matrix resolution of  $1,600 \times 1,200$  pixels with a pixel pitch of  $4.4 \mu\text{m}$ . A lens with a focal length of 16 mm was a compromise between the maximum coverage area of the rotor model and the measurement error. The cameras were synchronized by a system that provided simultaneous readings (moments of image recording). However, there was no synchronization with the rotation of the rotor, so random azimuthal positions of the blade were recorded. The information from the cameras was transmitted via an Ethernet channel which ensured the transmission of images to the computer via a cable of almost unlimited length, which is of great importance in aerodynamic experiment conditions. Images were collected by a computer with a gigabit network interface.

### 3. Experimental results

The experimental result processing program generated a graphic representation of the movement of both individual blade sections and three-dimensional forms of rotor flapping. An example of graphic representation of the movement of individual blade sections in the oblique flow mode at  $V=38$  m/s,  $n=433$  rpm with a thrust of  $T=800$  kgf is shown in Fig.3. The data are given for five sections located on relative radii  $r/R=0.226$ ; 0.398; 0.603; 0.798; 0.988. The dots mark the positions of the flexural axis of the sections at the moment of image recording and the solid line marks the Fourier first level approximation of the motion:  $y=y_0+y_1\sin\psi+y_2\cos\psi$ . The coefficients of the Fourier approximation  $y_0$ ,  $y_1$ ,  $y_2$  are given in Table 1.

Table 1

| $r/R$ | $y_0$   | $y_1$  | $y_2$   |
|-------|---------|--------|---------|
| 0.226 | 55.027  | 7.948  | 0.064   |
| 0.398 | 96.720  | 12.435 | -0.855  |
| 0.603 | 144.430 | 12.843 | -4.844  |
| 0.798 | 187.974 | 8.975  | -11.232 |
| 0.988 | 229.677 | 3.548  | -18.397 |

Figure 4 shows as an example a 3D graphical representation of the motion mode of the blade in flight mode at  $V=38$  m/s,  $n=433$  rpm,  $\alpha=-5^\circ$  and two rotor thrust values  $T=600$  kgf and  $T=800$  kgf.

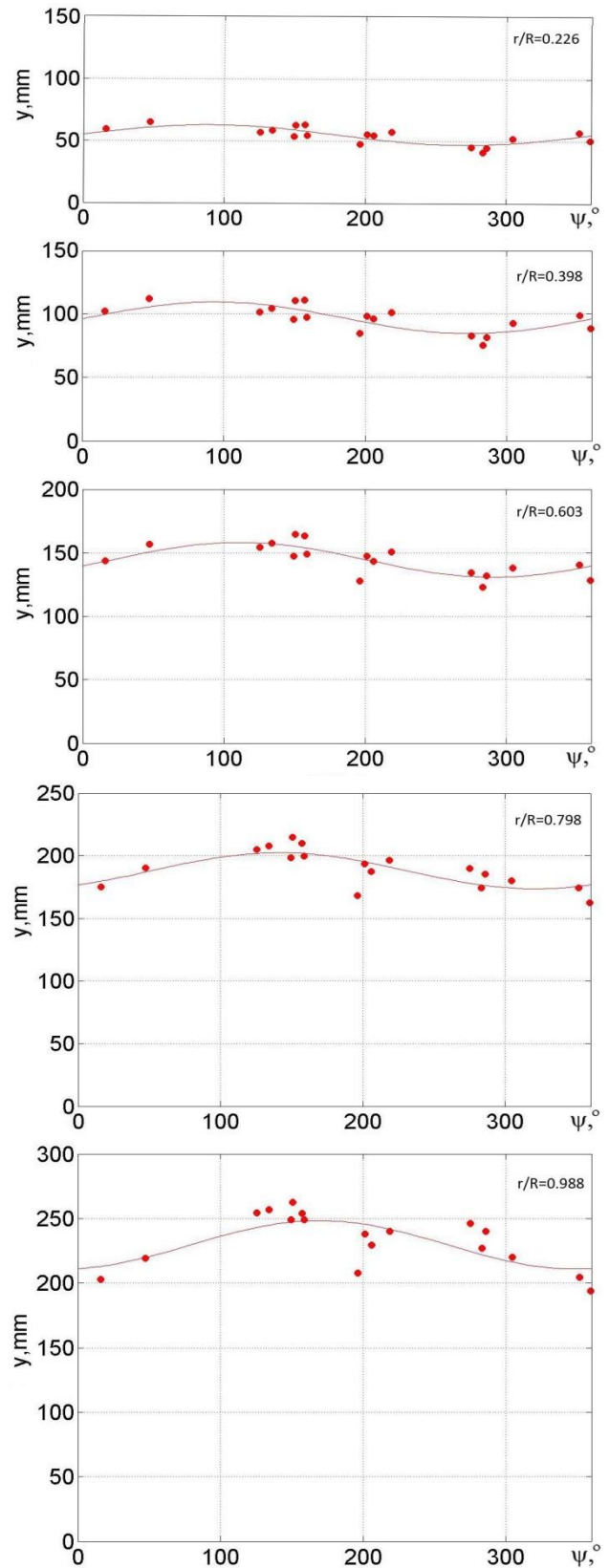


Fig. 3 Diagrams of flapping of blade sections

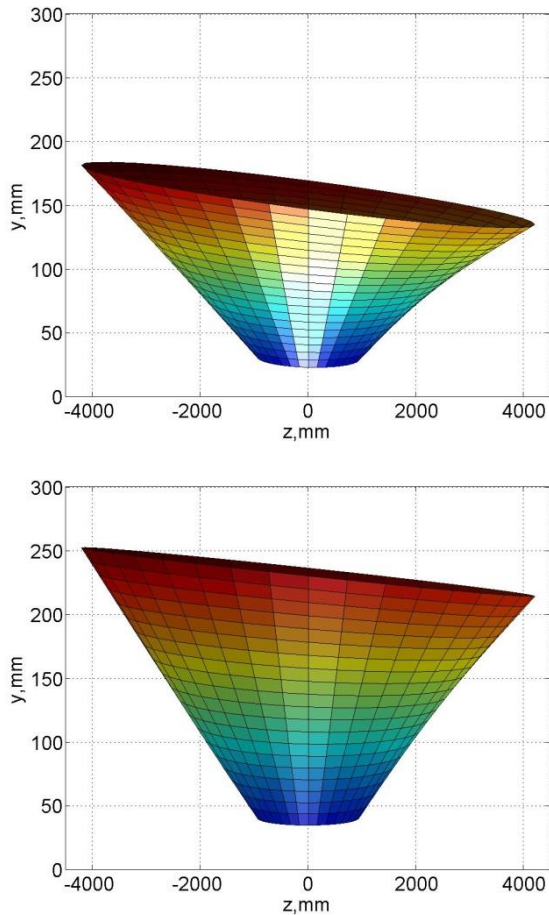


Fig. 4 Graphic representation of the motion mode of the blade.

#### 4. Calculation of the aerodynamic and dynamic characteristics of the main rotor

##### 4.1 Calculation method

In accordance with the unsteady nonlinear rotor blade theory based on a thin bearing surface [4,5], rotor blades are simulated by infinitely thin base surfaces the planform of which coincide with that of the blades and which are curved according to the law of curvature of the middle surfaces of the blades. An ideal incompressible medium is considered. The flow outside the rotor blades and their wakes is considered vortex-free.

The following boundary conditions are satisfied: the impermeability condition on the bearing surfaces; when passing through the surface of the

vortex wake, the conditions for continuity of pressure and normal velocity component are observed; on the rear edges of the bearing surfaces from which the vortex surfaces flow down, the Chaplygin-Zhukovsky hypothesis of stagnation is fulfilled; at an infinite distance from the rotor, as well as its wake, the perturbations converge.

Discretization in space and time is the numerical problem-solving procedure for the rotor in the nonlinear unsteady formulation according to the discrete vortex method. Continuous vortex layers that simulate the base surfaces of the rotor blades and their vortex wakes are replaced by discrete vortex frame systems, and the time-continuous process of changing boundary conditions and flow parameters is replaced by a stepped one. The values of the kinematic parameters remain unchanged within one-time step. At each time step, starting from the first one, after solving the system of equations to determine circulation, the intensity of all the vortex frames of the system of blades and the wake behind them are found. Summing up the aerodynamic load on the panels determines the distributed and total characteristics of the rotor. The wake shape is built up iteratively as a result of the calculation (Fig. 5).

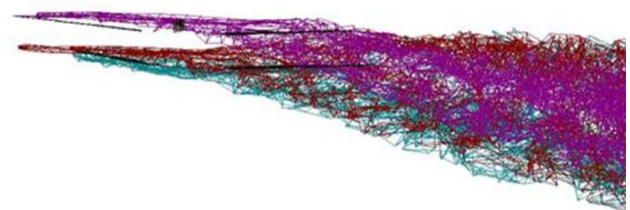


Fig. 5 Vortex wake structure behind a coaxial main rotor

##### 4.2. Simulation of the flow around a single three-blade main rotor

The flow around a three-blade main rotor of the helicopter, the geometric characteristics of which are given in Section 2, is considered. The kine-

matic parameters of the flow regimes are as follows: flow velocity  $V=38$  m/s, angle of attack of the rotor  $\alpha=-10$  degrees, tip speed  $\omega R=200.12$  m/s, pitch-flap coupling  $k=0$ .

For the 1st mode: the blade pitch angle  $\varphi=7.5$  degrees, the swash plate tilt  $\chi=1.1$  degrees (forward),  $\eta=0.2$  degrees (to the right), the rotor thrust  $T=830$  kgf. For the 2nd mode: the blade pitch angle  $\varphi=8.0$  degrees, the swash plate tilt  $\chi=0.96$  degrees (forward),  $\eta=0.21$  degrees (to the right), the rotor thrust  $T=900$  kgf.

Tests of the main rotor in the T-101 wind tunnel allowed obtaining the characteristics of the centrifugal motion of the blades which are presented as a vertical movement of blade sections relative to the plane of rotation of the rotor. The 5th section located almost at the blade tip ( $r_5/R = 0.988$ ) was mainly considered. Figure 6 shows the experimental points of vertical displacement of the 5th blade section for the considered 1st test mode. The approximation function  $y=y_0+y_1\sin\psi+y_2\cos\psi$  is also shown here where  $y_0, y_1, y_2$  are the Fourier approximation coefficients. In this case  $y_0=210.506$ ;  $y_1=5.223$ ;  $y_2= -26.093$ .

The experiment uses a non-standard reference system of the blade azimuth angle. The initial azimuth is taken in front of the rotor disk (Fig. 2b), therefore the blade at azimuth  $\psi=90$  degrees is flown around like a retreating blade. Therefore, when compared with the calculation results, the experimental points were recalculated to new azimuths ( $360 - \psi$ ). Figure 7 shows the same graph flipped vertically. Here the zero azimuth is counted from the left on the x-axis.

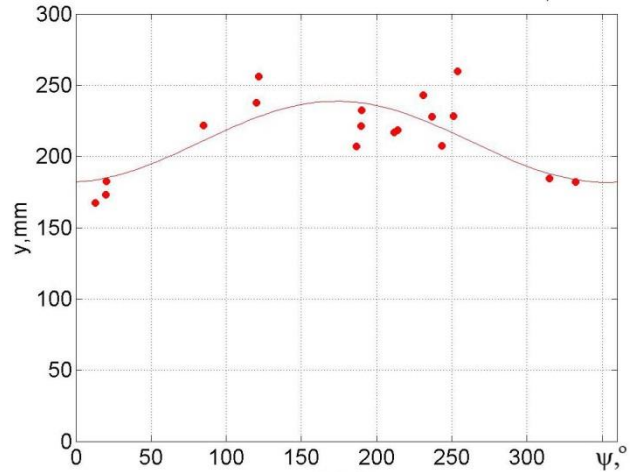


Fig. 6 Flapping characteristics of the 5th blade section for mode 1

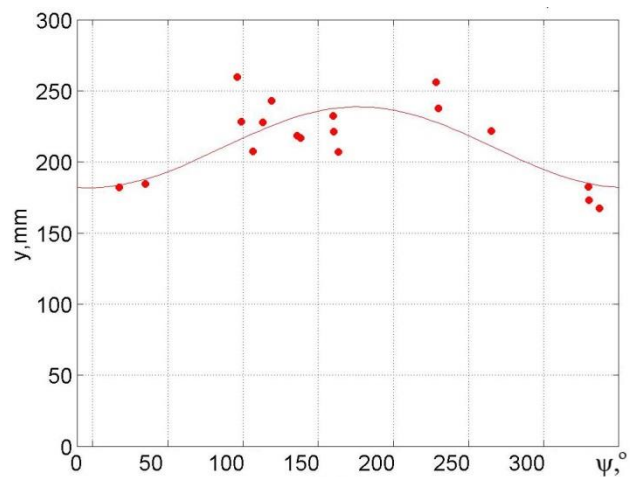


Fig.7. The graph shown in fig. 6 flipped vertically

Processing the experimental points in the new coordinate system (azimuthal position of the blade) and comparing with the approximation function  $y=y_0+y_1\sin\psi+y_2\cos\psi$  and the calculated curve give the following picture (Fig. 8).

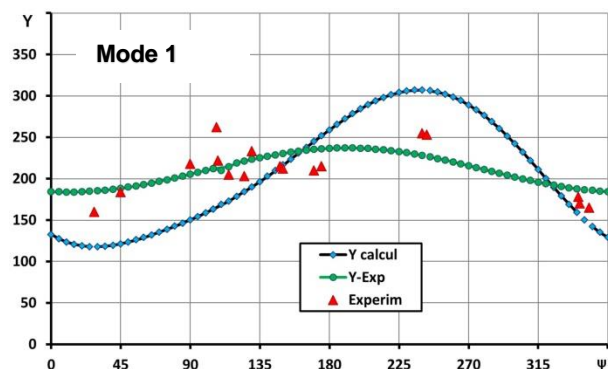


Fig. 8 Comparison of calculated and experimental data on rotor flapping for mode 1

For mode 2 of rotor tests, similar data is as follows (Fig. 9-10).

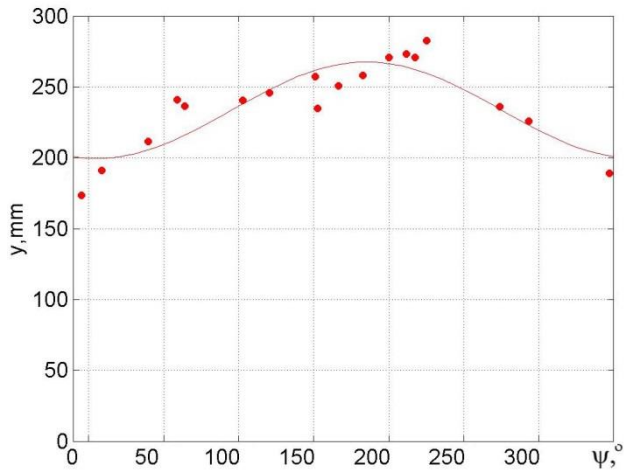


Fig. 9 Experimental flapping characteristics of the 5th blade section for mode 2

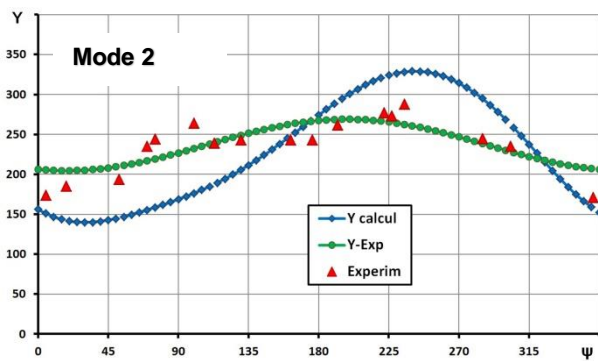


Fig. 10 Comparison of calculated and experimental data on rotor flapping for mode 2

Analysis of the graphs shows that while maintaining the tendency of the vertical coordinate  $Y$  of the 5th tip section of the blade to change, the value of  $Y$  is overestimated in the calculations when the blade flaps upstroke and underestimated when it flaps downstroke. The reason for this seems to be that the calculations use a model of horizontal hinge in which there is no friction, the blade takes its position under a set of forces, and in the experiment the blade is attached to the hub by a torsion which has a damping effect when deformed. With increasing rotor thrust, both in the calculation and in the experiment, the vertical coordinate increases, i.e. the blade flapping angle increases.

### 4.3. Calculation studies of the effect of the mutual arrangement of the blades of a coaxial main rotor

The coaxial helicopter must exclude collision of the blades of the upper and lower rotors during flight operations, to reduce the vibrations due to rotor pulsations, and to reduce the noise generated mainly by the coaxial main rotor (MR). It is found that the initial azimuth, e.g., of the upper rotor blade, which does not coincide with the initial azimuth of the lower rotor blade, affects the above-noted features of the coaxial helicopter.

Numerical studies were performed to assess the effect of the initial azimuth of the upper rotor blade on the thrust pulsation of the coaxial helicopter MR. The studies were carried out using the calculation method specified in Section 2.1 [4,5].

Flow around a six-bladed coaxial MR (two rotors with 3 blades each, the geometric and mass-inertial characteristics of which are the same as in the previous sections) in the oblique flow mode at speeds  $V_1=51.25$  m/s (rotor angle of attack  $\alpha_1 = -5$  degrees) and  $V_2=71.75$  m/s ( $\alpha_2 = -12$  degrees) were considered.

Simulation of the non-stationary flow around the MR starts from the moment when the blade of the lower rotor takes the initial position with azimuth  $\psi=0$ . At that moment, the blade of the second upper rotor can occupy a position with a non-zero azimuth, for example, shifted by some angle  $\Delta\psi$ , which is conventionally called "phase" or "phasing" (Fig. 11). The lower 1st rotor rotates counterclockwise when viewed from above, and the 2nd upper rotor rotates clockwise. Depending on the phase  $\Delta\psi$  during rotation, the blades of the upper and lower rotors intersect at different points in time.

It is found that the phase  $\Delta\psi$  affects the nature of the approach of the upper and lower rotor blades of the coaxial MR, as well as the thrust pulsation and the rotor loading noise. Here, the effect of the phase  $\Delta\psi$  of the upper screw on the thrust pulsation of the coaxial helicopter MR is

estimated. The variation of the MR thrust coefficient  $C_T$  in one revolution was studied at  $\Delta\psi = 0, -20, -30, -40, -60, -80, -100, -120$  degrees.

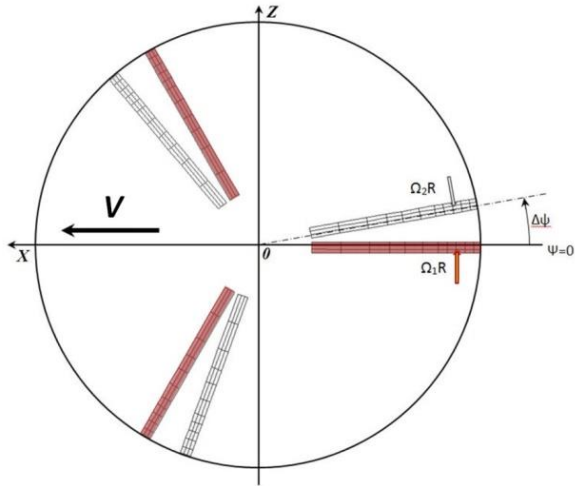


Fig. 11 Initial azimuth of MR blades

The thrust coefficient of the coaxial MR  $C_T$  is determined by summing the thrust coefficients, respectively, of the lower  $C_{TL}$  and the upper  $C_{TU}$  rotors. E.g., at a speed of  $V=51.25$  m/s, when  $\Delta\psi = 0$ , the increments of thrust coefficient of the

lower and upper rotors increase the thrust pulsations (Fig. 12, a), while at  $\Delta\psi = -60^\circ$ , the pulsation peaks of the upper and lower rotors are shifted and the total thrust coefficient of the coaxial MR  $C_T$  changes in one turn with a smaller amplitude (Fig. 12, b).

Figure 13a shows the results of the calculation of thrust coefficient pulsations of the coaxial MR  $\Delta C_T = C_{TMAX} - C_{TMIN}$  for two flow velocity values  $V_1=51.25$  m/s ( $V_1/\omega R=0.25$ ) and  $V_2=71.75$  m/s ( $V_2/\omega R=0.35$ ) and Figure 13, b shows the thrust pulsations for the same velocities as a percentage of the mean  $C_T$  value.

Analysis of these results allows assessing the effect of the initial azimuth of the upper rotor blades  $\Delta\psi$  on the thrust pulsation of the helicopter coaxial MR without damping. In particular, when the initial azimuth of the upper rotor blades approaches zero, the maximum values of thrust pulsation occur, which, for example, at a flow velocity  $V_2=71.75$  m/s, exceeds 35% of the mean  $C_T$ , and the minimum of thrust pulsation is when  $\Delta\psi \approx 60^\circ$ .

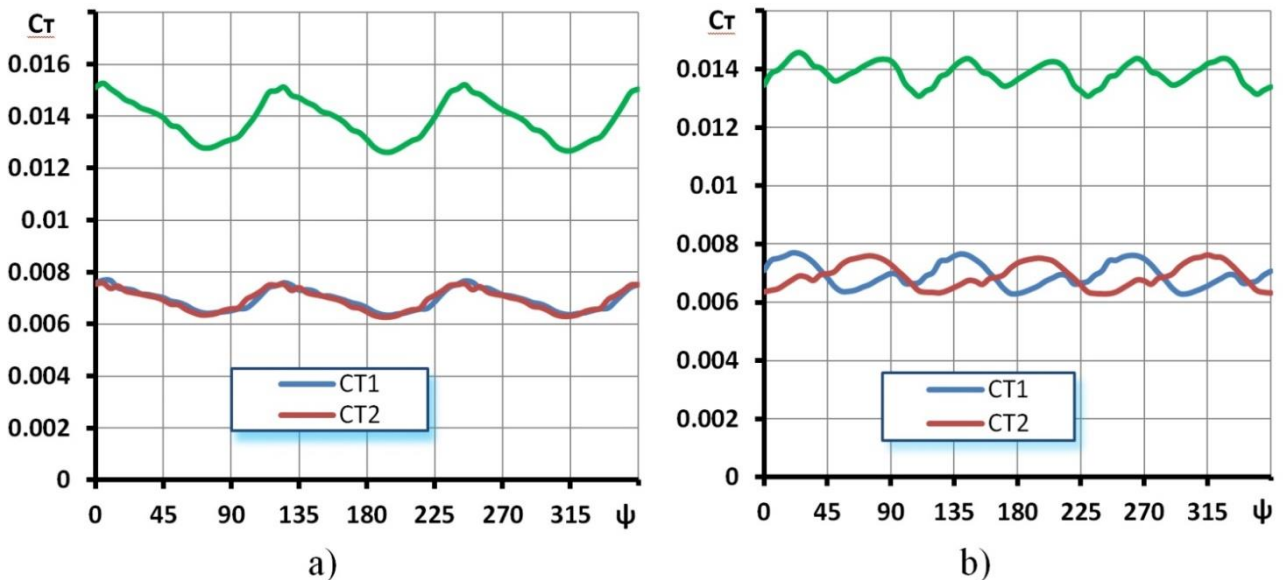


Fig. 12 Change in the rotor thrust coefficient in one revolution with  $\Delta\psi = 0$  (a) and  $\Delta\psi = 60^\circ$  (b)

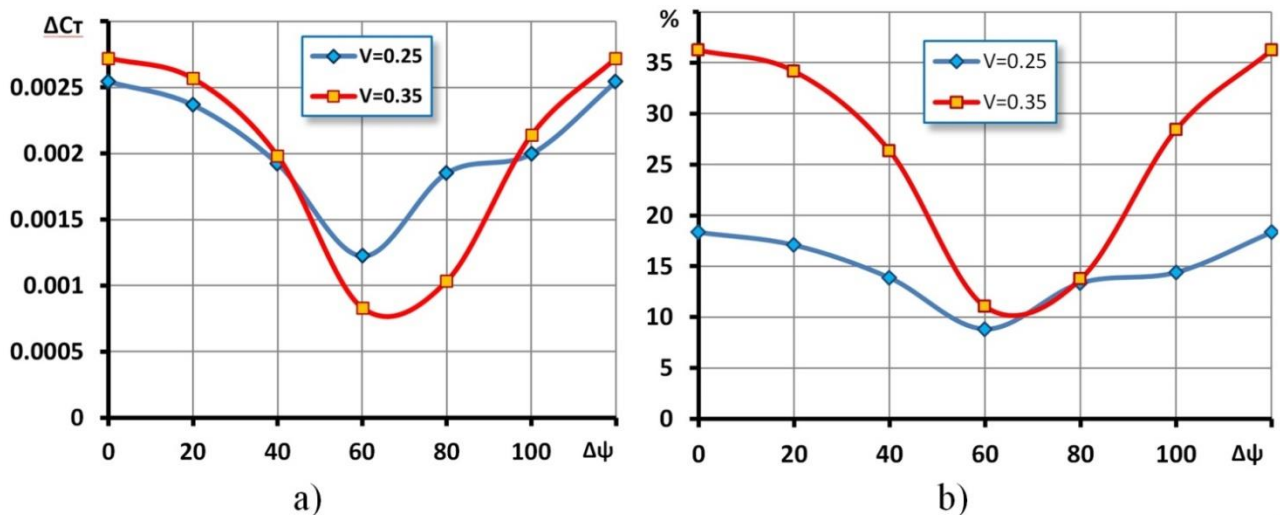


Fig.13 Effect of the phase on the change in the thrust coefficient  $C_T$  (a) and the amplitude of thrust pulsation of the coaxial MR as a percentage of the mean value  $C_T$  (b)

Analysis of these results allows assessing the effect of the initial azimuth of the upper rotor blades  $\Delta\psi$  on the thrust pulsation of the helicopter coaxial MR without damping. In particular, when the initial azimuth of the upper rotor blades approaches zero, the maximum values of thrust pulsation occur, which, for example, at a flow velocity  $V_2=71.75$  m/s, exceeds 35% of the mean  $C_T$ , and the minimum of thrust pulsation is when  $\Delta\psi \approx 60^\circ$ .

## 5. Conclusions

Videogrammetry is an effective tool for the experimental study of the motion and deformation of a helicopter rotor blade.

Calculation of the flapping characteristics of the blades of a hinged rotor without taking into account the torsion gives overestimated results.

The initial azimuth, e.g., of the upper rotor blade, which does not coincide with the initial azimuth of the lower rotor blade, affects the thrust pulsations of the rotors of a coaxial helicopter.

## References

[1] Inshakov S.I., Kulesh V.P., Mosharov V.E., Radchenko V.N. Videogrammetry method of non-contact measurements of instantaneous

deformation of rotating propellers blades. // TsAGI Science Journal. – 2013. Vol. XLIV, Issue 4. – P. 72– 79 (In Russian).

[2] Bosnjakov S.M., Kulesh V.P., Fonov S.D. et al. Videogrammetric system for studying of movement and deformation of real– scaled helicopter rotor blades. // SPIE. – 1999. Vol. 3516, 0277– 786X/99, Part One, P.196– 209.

[3] Kulesh, V. P. Noncontact measurements of geometrical parameters of objects' shape, motion and deformation in experimental aerodynamics. // Datchiki & Systemi (Sensors & Systems). – 2004. Issue 3. – p. 22– 27 (In Russian).

[4] Belotserkovskii, S.M., Loktev, B.E., and Nisht, M.I. Computer-Aided Study of Aerodynamic and Aeroelastic Characteristics of the Helicopter Rotors. – Moscow: Mashinostroenie, 1992. – 218 p. (In Russian).

[5] Kritsky, B.S. Mathematical model of rotorcraft aerodynamics. Moscow State Technical University of Civil Aviation (MSTU CA), Civil Aviation High Technologies, Issue 59, series "Aeromechanics and Strength", 2003, p. 24-31 (In Russian).

## **Copyright Statement**

The authors confirm that they, and/or their company or organization, hold copyright on all of the original material included in this paper. The authors also confirm that they have obtained permission, from the copyright holder of any third party material included in this paper, to publish it as part of their paper. The authors confirm that they give permission, or have obtained permission from the copyright holder of this paper, for the publication and distribution of this paper as part of the ERF proceedings or as individual off-prints from the proceedings and for inclusion in a freely accessible web-based repository.